

Energy-gain spectroscopy studies of electron capture from helium by slow multiply charged neon ions

C. Schmeissner, C. L. Cocke, and R. Mann*

J. R. Macdonald Laboratory, Physics Department, Kansas State University, Manhattan, Kansas 66506

W. Meyerhof

Department of Physics, Stanford University, Stanford, California 94305

(Received 2 April 1984)

Energy spectra of the projectile ions have been measured following electron capture by slow Ne^{q+} ions on He for $3 \leq q \leq 8$. Both single-capture and transfer ionization were observed. The reactions are all exoergic with positive energy defects between 3.6 and 31 eV, and with crossing radii between 8 and 2.1 Å. Capture is found to selectively populate states whose crossings lie at a radius which can be calculated on the basis of a simple prescription. The total transfer cross sections range up to 55% of the geometrical ones deduced from the measured crossing radii.

I. INTRODUCTION

The capture of an electron from a neutral target by a multiply charged projectile whose velocity is much less than that of the target electron is usually described as proceeding via localized crossings between potential curves of the incident channel with the Coulomb-promoted exit channel. By this mechanism only exoergic reaction channels can be fed, with the positive energy defect (Q) increasing the translational kinetic energy of the collision partners. Excited states with the electron in a high- n level about the projectile core are selectively populated in the process. A great deal of theoretical and experimental work on the process has now been reported¹⁻⁴ and several discussions of the relevance of the process to applied concerns have been given.^{5,6}

Most of the experimental work deals with total cross sections which integrate over all final states. Information on the specific final states populated has come from translational energy spectroscopy of the reaction products and from photon and electron spectroscopy of the final states. A high n selectivity was found early in the K x-ray and Auger-electron spectroscopy of neon on various targets by Mann *et al.*⁷ and Beyer *et al.*⁸ where capture onto metastable cores of Ne was used to produce fast electrons and similar hard radiation from capture to bare O and C nuclei has been reported by Bliman *et al.*⁹ Softer photon spectroscopy has recently allowed both n and l differentiation of final states for O^{q+} , C^{q+} , and Ne^{q+} projectiles on He and Li for q up to 8.^{10,11}

Translational energy spectroscopy has been carried out by the Nagoya group¹²⁻¹⁵ for C^{q+} , N^{q+} , O^{q+} , and Ne^{q+} on He at projectile energies near $1 \text{ keV} \cdot q$ for $q \leq 9$ and by Mann *et al.*¹⁶ for Ne^{9+} and Ne^{10+} on various targets at projectile energies of $50 \text{ eV} \cdot q$.¹⁵ Huber, Kahlert, and collaborators¹⁷⁻¹⁹ have reported high-resolution translational energy spectroscopy for multiply charged rare-gas Ne projectiles Ar on rare-gas targets, as have Kamber and Hasted²⁰ and Nielsen *et al.*²¹

A consistent picture of highly selective capture to excit-

ed states emerges from the above results. The most commonly used model for predicting the n value populated is the classical over-barrier model,^{8,22} which has been quite successful.

In this paper we present a systematic study of electron transfer in slow Ne^{q+} on He collisions for q between 3 and 8. When combined with the results of Mann *et al.*,¹⁶ these data complete the systematics for this system for all projectile charge states above 2. Both intermediate resolution translational energy spectra of the neon projectiles, referred to hereafter as energy-gain spectra, and total transfer cross sections are now available. The intent is to provide a comprehensive study of the states populated and the transfer probabilities for a single system from a low charge state (for which capture is quite weak) to the bare nucleus.

II. EXPERIMENT

The neon ions were produced in a secondary ion recoil source by pumping a dilute neon gas with fast fluorine

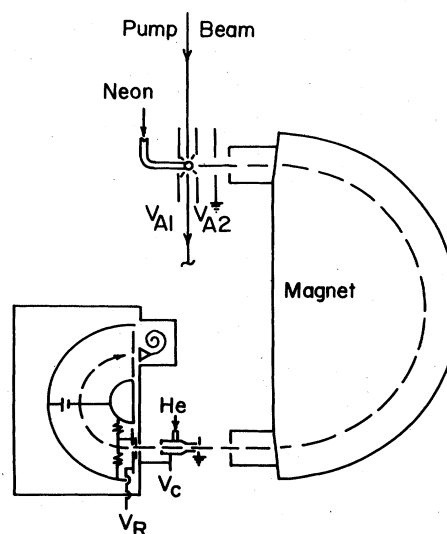


FIG. 1. Schematic of apparatus.

and iodine beams from the KSU tandem. The source is discussed in detail elsewhere.²³ The extracted neon ions were charge-state and momentum analyzed by a double-focusing magnetic spectrometer with a momentum resolution $\Delta p/p$ of 1.2% and directed into a He gas cell 2 cm long (see Fig. 1). The entrance and exit apertures of the cell were 2 and 3 mm in diameter, respectively. Ions exiting the cell passed through a short retardation system into a hemispherical electrostatic analyzer which analyzed the energy and charge state of the post-collision projectile ions. Target pressures were typically below 1 mTorr, with a background pressure in the chamber of 2×10^{-6} Torr.

The effective extraction voltage V_0 in the primary cell was set near 25 V, limiting the energy spread of the incident neon beam to $\Delta E_B = 0.6 \text{ eV} \cdot q$, where q is the neon charge state. The collision energy was varied by applying a variable negative voltage of size V_c to the gas cell. The collision energy was then given by $V_{\text{acc}}q$, where the effective acceleration potential $V_{\text{acc}} \equiv V_c + V_0$. The ions were retarded after leaving the cell by applying a voltage V_R to the entrance slits of the hemispherical analyzer. The analyzer was operated at a fixed plate voltage so as to pass ions having an energy of $12.5 \text{ eV} \cdot q'$, where q' is the charge state of the neon after the collision. The overall energy resolution for the direct beam was expected to be less

than $0.7 \text{ eV} \cdot q$; measured values ranged from 0.4 to 0.6 $\text{eV} \cdot q$ for cell voltages below 120.9 V. For large cell voltages, and correspondingly large retardation factors, the measured resolution deteriorated, reaching $2 \text{ eV} \cdot q$ at $V_c = 500 \text{ V}$. We attribute this deterioration to aberrations in the hemispherical analyzer, since for large retardation factors the angular divergence of ions inside the analyzer becomes large. The energy resolution per charge expected for charge exchange to a single final state, in the absence of kinematic broadening, can be shown to be close to that for the direct beam.

In most cases, the resolution of final states is limited by kinematic effects. At scattering angles other than 0° some energy is carried away from the collision by the helium recoil, and the energy gained by the projectile is a function of scattering angle. The acceptance angle of the analyzer was sufficiently large that, in most cases, all of the reaction products of interest were accepted (see below). Within this acceptance window, however, lie an appreciable range of scattering angles and a corresponding range of energy gains. We have estimated the size of this effect using a model whereby the neon projectile is assumed to follow a classical trajectory through the collision. Under such conditions, every impact parameter (b) corresponds to a unique scattering angle (θ) with the relationship de-

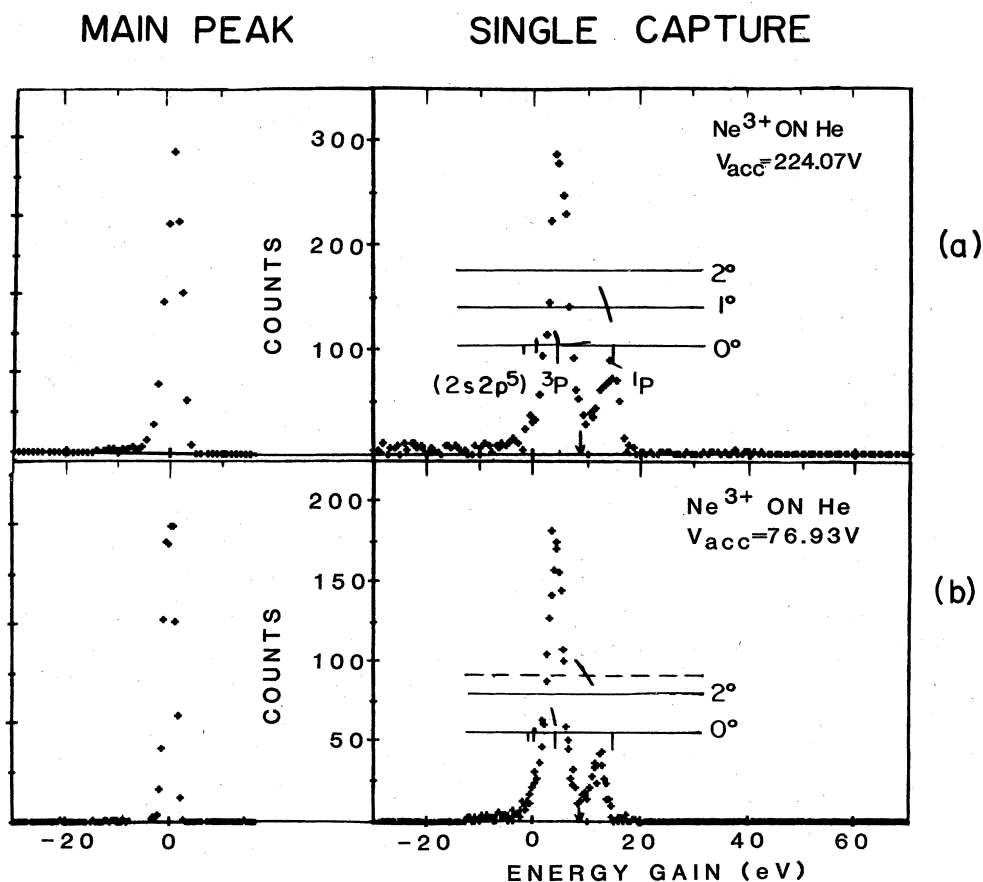


FIG. 2. Energy-gain spectrum for single capture by Ne^{3+} on He at projectile energies of 224.07 and 76.93 $\text{eV} \cdot q$. The favored Q_f calculated according to the prescription in the text is indicated by vertical arrows.

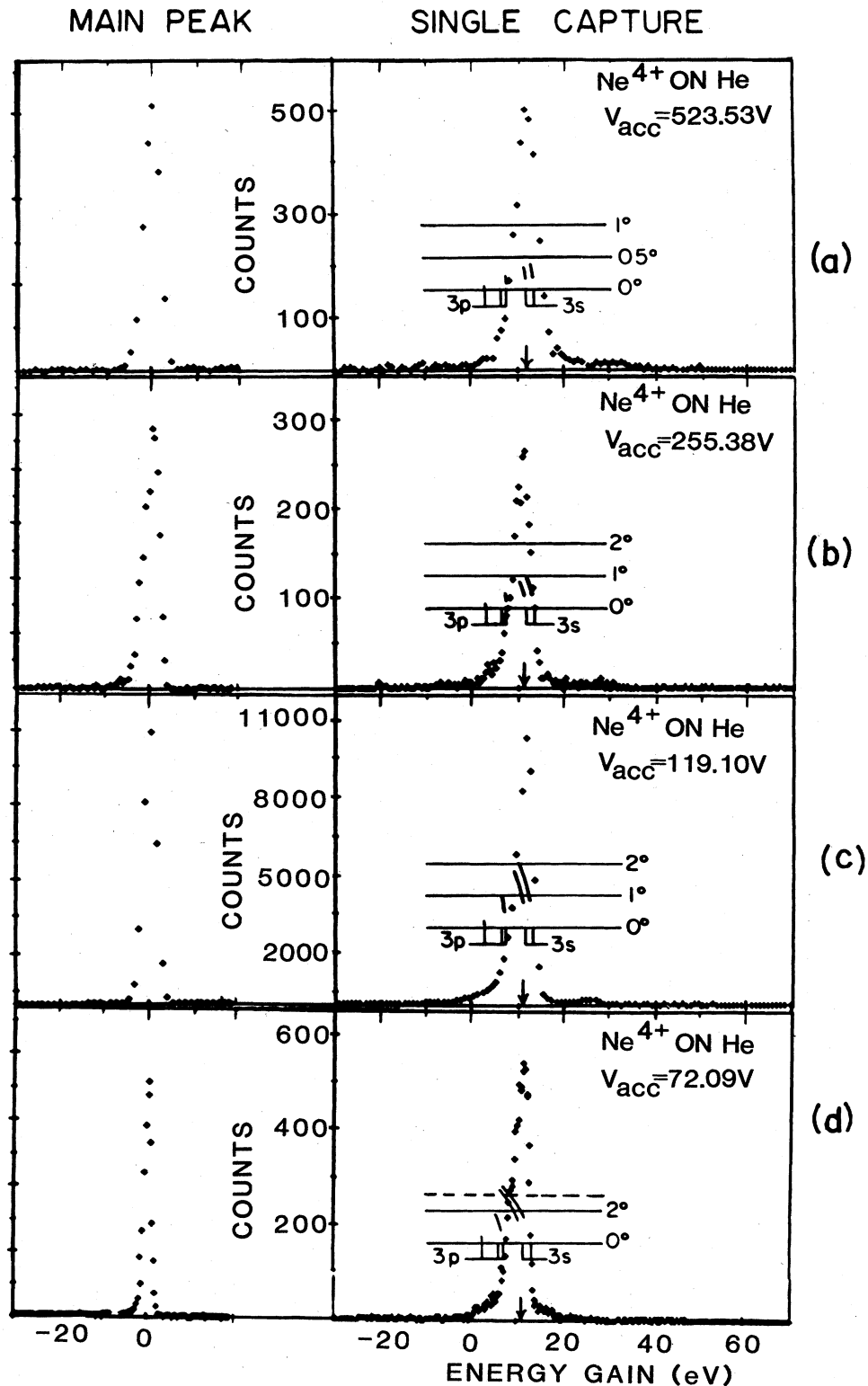


FIG. 3. Similar to Fig. 2, but for Ne^{4+} on He.

pending on the potential curve which the system follows through the collision. The electron transfer was taken to proceed at a localized crossing between incident and final potential curves, leading to a minimum scattering angle

corresponding to a collision for which the impact parameter is just equal to the crossing radius R_c . This scattering angle was calculated on the assumption that the projectile of charge q proceeded undeflected to an internuclear

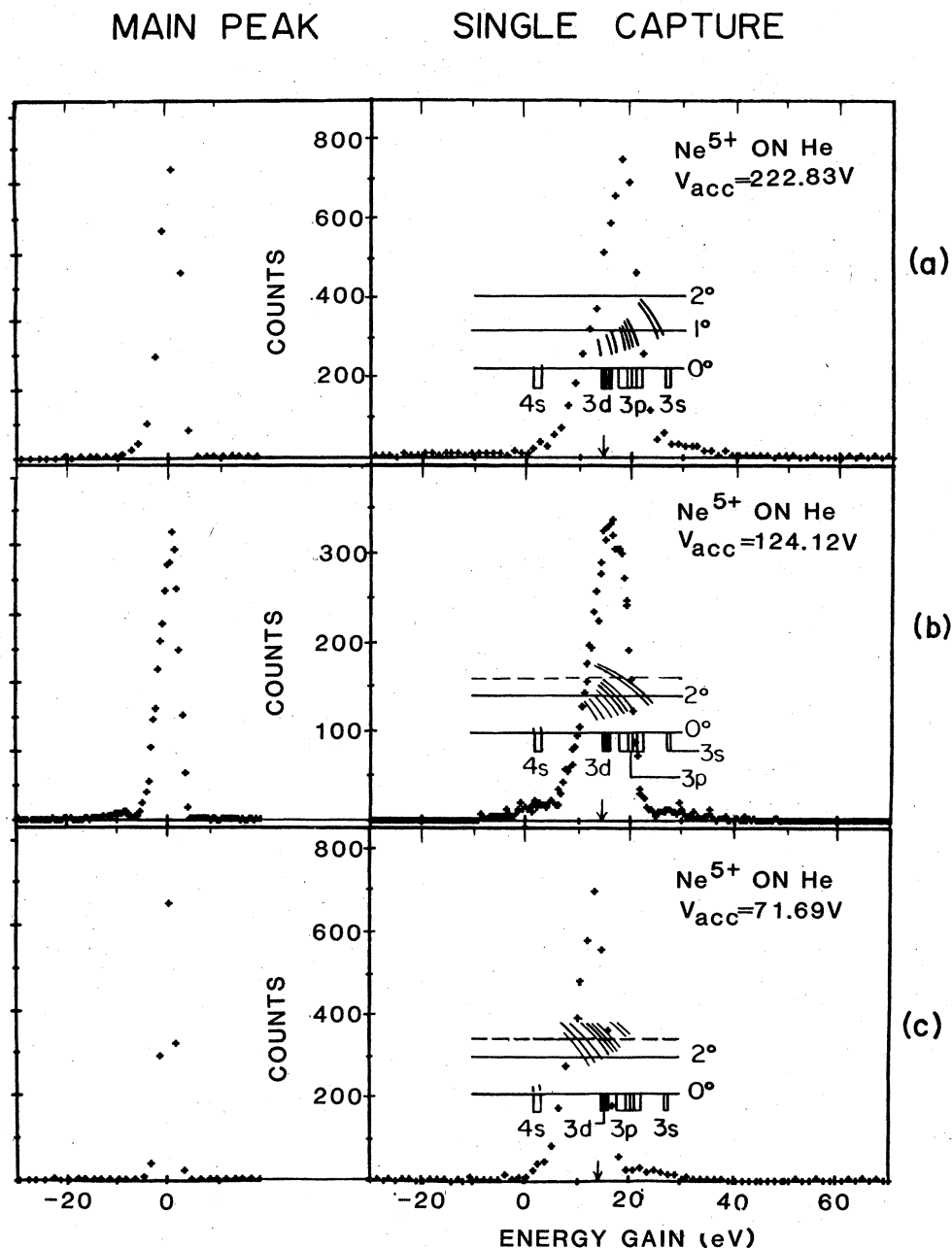


FIG. 4. Similar to Fig. 2, but for Ne^{5+} on He.

separation of R_c (half-Coulomb scattering model) and then exited on a Coulomb trajectory characterized by neon and helium charge states of $(q-1)$ and 1, respectively (for single capture). The radius R_c is related to the Q value for the reaction by $R_c = [(q-1)e^2]/Q$.

In order to display the kinematic effect, we show, in Figs. 2–7, line segments showing the projectile energy gain versus laboratory scattering angle for a selection of a final state. The kinematic lines are calculated from standard two-body kinematics. They have been truncated on the low-angle side at the minimum scattering angle calculated as described above. On the large-angle side, a trun-

cation was made at an angle corresponding to a trajectory with an impact parameter of $b = R_c/2$, where the half-Coulomb scattering model was again used. While in reality the kinematically determined maximum scattering angle is much larger, one would expect most of the cross section to lie between R_c and $R_c/2$. The kinematic effect can be quite large, especially for small bombarding energy or for large Q , and in some cases essentially renders impossible our observation of capture to states involving very large energy releases.

The angular acceptance of the analyzer was investigated by numerically solving Laplace's equation and integrating

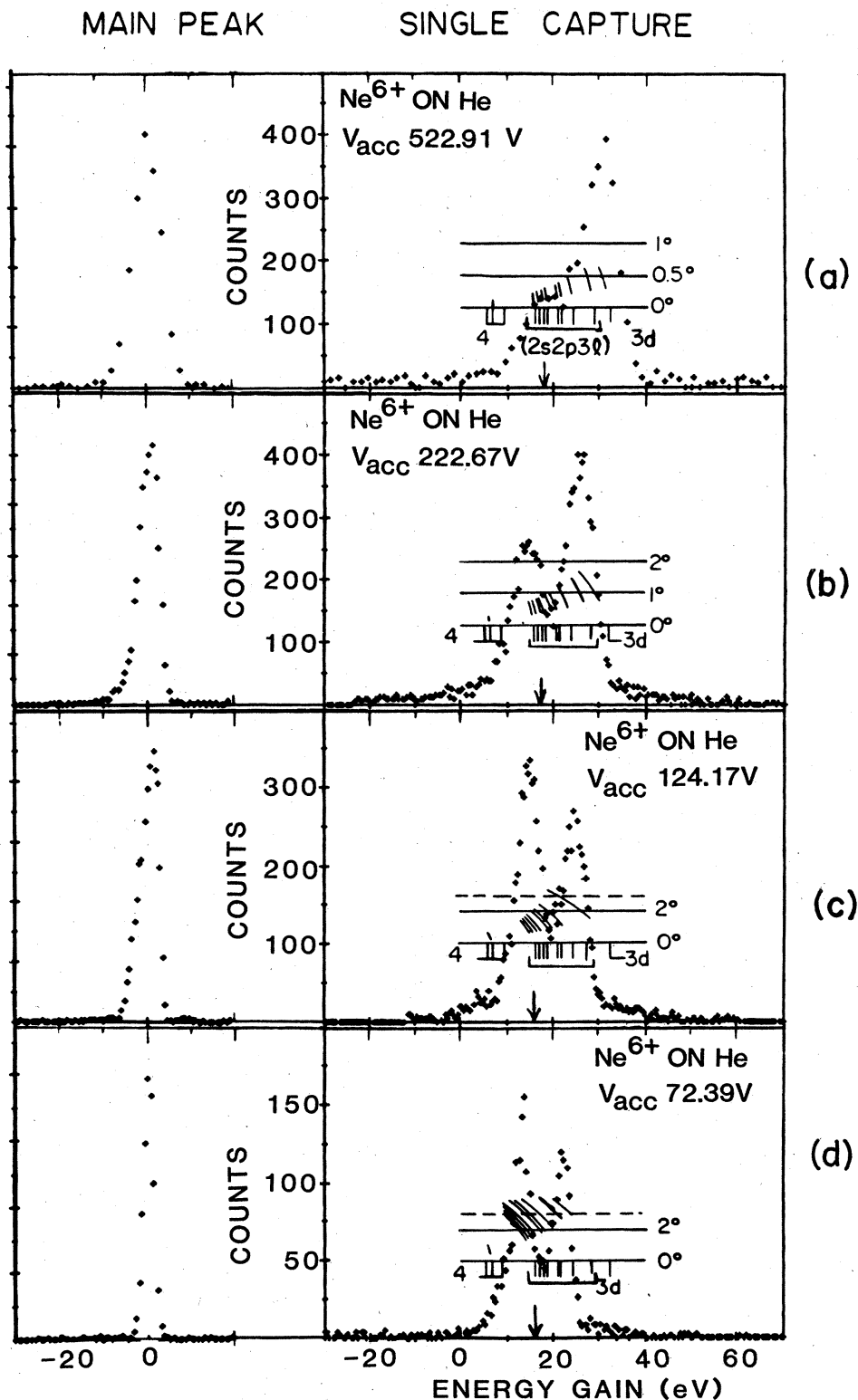


FIG. 5. Similar to Fig. 2, but for Ne^{6+} on He. States indicated by $(2s\ 2p\ 3l)$ are core excited.

the equations of motion for an ion traversing the geometry of the retarding lens system and spectrometer. These calculations showed that, for a parallel incident beam and no cell voltage, ions scattered near the cell

center through an angle less than approximately 2.8° will be accepted by the spectrometer. This result is nearly independent of the retardation factor, a surprising but convenient feature which occurs because of the shortness of

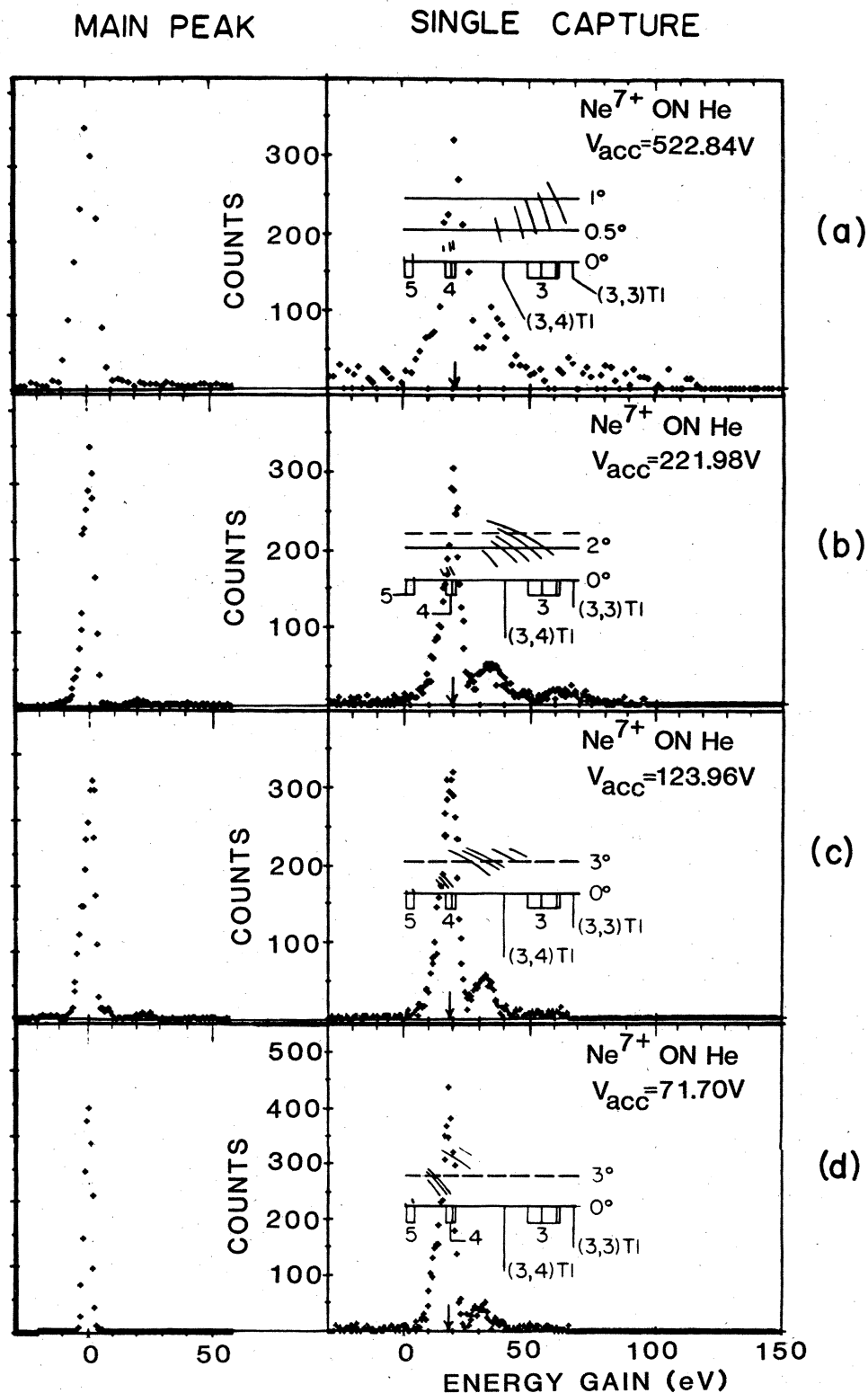


FIG. 6. Similar to Fig. 2, but for Ne^{7+} on He. The notation (n, n') TI refers to transfer ionization proceeding through doubly excited states with electrons in shells denoted by n and n' .

the retarding lens. This cutoff angle is indicated by a dashed line in the figures. In some cases, the large-angle limit deduced from the kinematic exceeded 2.8° , and we have truncated the kinematic line segments slightly

beyond 2.8° for these cases. Larger-angle events are lost from our analyzing system, and we measure only partial cross sections for such cases. Experimental evidence is seen for this cutoff angle in Figs. 3 and 6 and is discussed

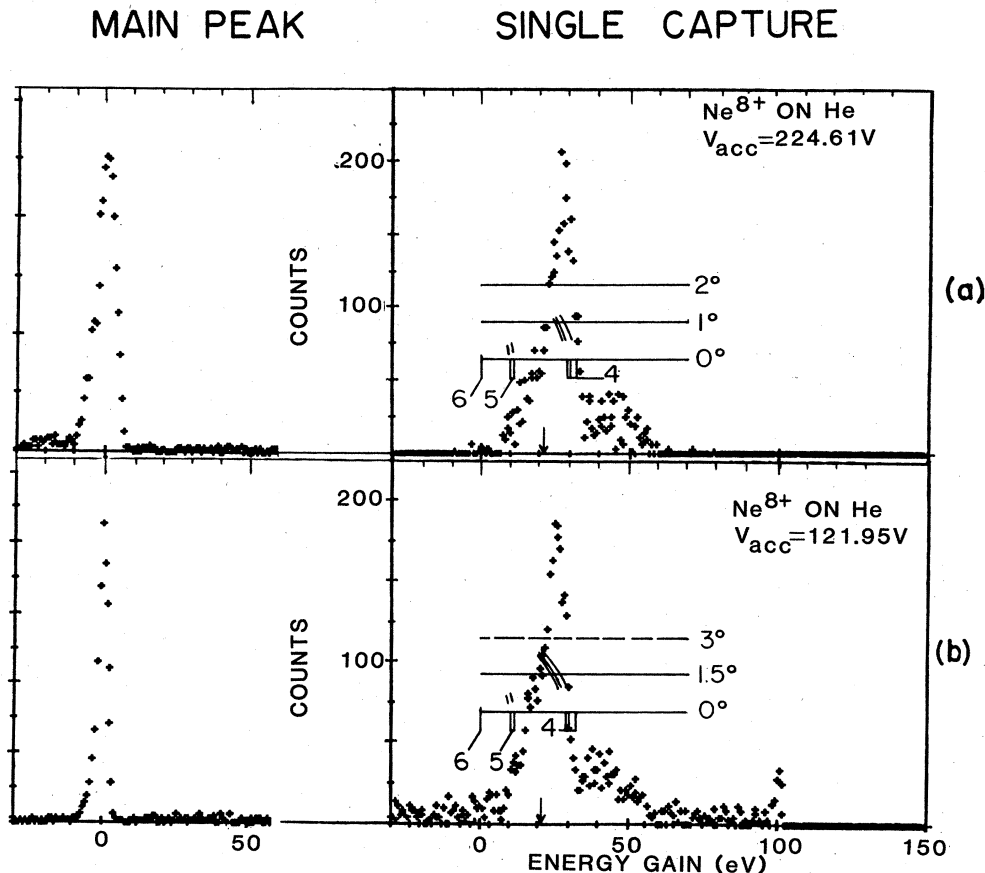


FIG. 7. Similar to Fig. 2, but for Ne^{8+} on He.

further below.

Investigation of effects of the lens created at the cell entrance by the cell voltage showed that, for V_{acc} less than 120 V, the 2.8° cutoff remains approximately valid. For $V_{\text{acc}} = 220$ and 520 V, the beam converges sufficiently close to the cell entrance that the spectrometer samples a wide range of scattering angles with nearly equal weight, thus making the effective cutoff angle larger, although at cost in transmission efficiency. For such large V_{acc} cases, however, the capture events are sufficiently forward directed that we do not expect cutoff effects to be large.

Spectra were taken by scanning the retardation voltage V_R . The energy gain E_G corresponding to V_R is given by $E_G = q'(V_R - V_R^0) + (V_{\text{acc}})(q' - q)$, where V_R^0 is the retardation voltage for which the main beam is passed. The retarding voltages were measured with digital and differential voltmeters, and V_{acc} was determined with the use of the experimentally determined spectrometer calibration constant. Events corresponding to $q' = q$ are separated from single-capture events with $q' = q - 1$ by lying in a different portion of the V_R spectrum. Double-capture events were not sought, since this channel is known to be weakly fed in most cases.²⁴

III. RESULTS AND DISCUSSION

A. General features

Energy-gain spectra are shown in Figs. 2–7. Due to the kinematic effect discussed above, identifications must

be made by associating observed peaks with the kinematic line segments, rather than unique energy gains. Each kinematic line segment is identified on the 0° intercept by the state whose population it represents. A simplified notation is used on the figures to indicate only the n , and sometimes l , of the captured electron. Only states based on the ground-state projectile core are so identified in the figures. Core excited states are important for the cases of Ne^{3+} and Ne^{6+} projectiles, and in these cases the full electronic configuration is given. The energies are taken from Refs. 25 and 26, and channels leading to excited He^+ are not considered since they are not expected to be strongly populated and in most cases do not lie in the interesting regions.

Before entering a discussion of the individual collision systems, it is useful to discuss some general features which are expected to determine which capture channels will be most strongly fed. For the low velocities used here, capture may be expected to proceed at localized crossings between the incident $\text{Ne}^{q+} + \text{He}$ channel and the final $\text{Ne}^{(q-1)+} + \text{He}^+$ systems. When only a single exit channel is available with a crossing at R_c , a Landau-Zener treatment of the process²⁷ gives a maximum cross section if the potential coupling matrix element $H_{12}(R)$ between incident and exit channels, evaluated at the crossing radius, has a magnitude given by

$$|H_{12}(R_c)|^2 = 0.42v_0 \Delta F / 2\pi, \quad (1)$$

where v_0 is the projectile velocity and ΔF is the derivative with respect to internuclear radius of the energy difference between the two potential curves. (Unless otherwise indicated, atomic units are used throughout.) The transfer cross section under these optimized conditions is given by $\sigma = 0.452\pi R_c^2$. Several universal prescriptions for H_{12} , based on calculations for atomic hydrogens, have been given. We use that of Olson and Salop,²⁸ who find

$$H_{12}(R) = (\sqrt{2})9.73\sqrt{q} \exp(-1.32\alpha R/\sqrt{q}), \quad (2)$$

where $\alpha = \sqrt{2}I_t$ and I_t is the target ionization potential. We have inserted the $\sqrt{2}$ because there are two He electrons for this case. If polarization effects are ignored, $\Delta F = (q-1)/R^2$. By inserting Eq. (2) into Eq. (1), one can solve for a "favored" crossing radius R_f for which conditions for transfer are optimized; the corresponding favored Q value is given by $Q_f = (q-1)/R_f$. Because H_{12} is such a steep function of R , the values of R_f and Q_f thus obtained are not very sensitive to the leading numerical factor in Eq. (2). The R_f differs little from the "absorption" radius used by Olson and Salop²⁸ for cases discussed here. It is only very weakly dependent on the collision velocity. In Figs. 2–7 the results of the above prescription for obtaining Q_f are indicated by arrows on the energy axes.

For cases where a single channel is found experimentally to dominate the capture process, the energy-gain spectrum can be used to define an experimental crossing radius through $R_e = (q-1)/Q_e$ where Q_e is the experimentally determined Q value. By combining this with the experimental cross section σ_e we may define an average transition-probability parameter $\bar{P} \equiv \sigma_e/\pi R_e^2$. In a two-level Landau-Zener model, the maximum value of \bar{P} would be 0.452. In an absorbing sphere picture, with many crossings participating, one would expect \bar{P} to be near unity.

For the cases where two (or more) major groups are populated, the parameter \bar{P} is defined for each group by assigning to each a fraction of the cross section propor-

tional to its fractional population in the energy spectrum. In Table I we summarize major experimental results deduced from Figs. 2–7 and total capture cross section measurements.

In general, if several capture channels have crossings near the favored region of R , lowering the collision velocity will tend to enhance the population of those channels with larger crossing radii. This occurs because crossings at large R , with smaller H_{12} , will behave less diabatically the lower the velocity. This effect is exhibited in the above prescription by the moving of R_f outward, and Q_f to smaller values, as the collision velocity is lowered, although the arrows in Figs. 2–7 show this effect to be small. Unfortunately, the effect of the experimental angular cutoff acts in the same direction as this diabaticity effect. The lower the velocity, the more likely large- Q events are to be lost, thus enhancing the apparent relative population of low- Q channels. These two effects are not always cleanly separable in our spectra.

B. Discussion of individual collision systems

$Ne^{3+} + He$ (Fig. 2). For this system, the only states with the correct parent cores which can be populated exoergically are the 1D and 1S with Q values of 36.3 and 32.6 eV. These lie far from the favored Q region, and no evidence for their population is seen. The major capture channels appear to be the $^3P^o$ and $^1P^o$ states, both based on excited cores, lying at 14.1 and 3.6 eV, respectively. Values of \bar{P} for these channels are only 0.034 and 0.008, respectively, at $V_{acc} = 224.07$ V. These low values we attribute to the very weak coupling of the incident channel to core-excited configurations. The total cross section for capture is quite low for the same reason. The smaller relative population of the $^3P^o$ state at collision energy of 76.93 eV is due to the spectrometer angular cutoff as well as the diabaticity effect.

$Ne^{4+} + He$ (Fig. 3). The population of $n=3$ is now substantially exoergic. The $2s^22p^2(^3P)3s(^2,4P)$ states at

TABLE I. Summary of collision parameters for single capture for Ne^{q+} from He at a projectile energy of 220 eV $\cdot q$.

Projectile	$\sigma(10^{-16} \text{ cm}^2)$ total	\bar{Q} (eV)	$\sigma(10^{-16} \text{ cm}^2)$ partial	R_e (a.u.)	\bar{P}
Ne^{3+}	2.1 ± 0.3^a	14.1 ^b 3.62 ^b	0.45 ± 0.1 1.6 ± 0.2	3.86 15.0	0.034 ± 0.088 0.008 ± 0.001
Ne^{4+}	11.0 ± 1^b	11.5 ± 1^b	11.5 ± 1	7.1 ± 0.61	0.26 ± 0.05
Ne^{5+}	15 ± 3^c	19 ± 2^b	5 ± 3	5.7 ± 0.6	0.52 ± 0.15
Ne^{6+}	11 ± 2^a	32.1 ^b 19 ± 2^b	6.9 ± 1.2 4.1 ± 0.8	4.24 7.1 ± 0.7	0.44 ± 0.07 0.09 ± 0.02
Ne^{7+}	19 ± 3^c	19.5 ± 1^b	19 ± 3	8.4 ± 0.4	0.32 ± 0.06
Ne^{8+}	18 ± 6^c	31 ± 1^b	18 ± 6	6.1 ± 0.2	0.55 ± 0.19
Ne^{9+}	10 ± 2.5^d	24.8 ± 2^d	10 ± 2.5	8.8 ± 0.7	0.15 ± 0.04
Ne^{10+}	16 ± 2^d	29 ± 3^d	16 ± 2	8.4 ± 0.9	0.26 ± 0.06

^aFrom Refs. 23 and 36, interpolated for $V_{acc} \approx 220$ V, excluding transfer ionization.

^bPresent mean values for $V_{acc} \approx 220$ V, excluding transfer ionization.

^cAverage of present values with those of Refs. 23 and 36, interpolated for $V_{acc} \approx 220$ V, excluding transfer ionization.

^dFrom Ref. 16, for $V_{acc} = 49.2$ V.

13.1 and 11.9 eV lie nearly at the favored Q value, and their population is seen to dominate for all accelerating voltages. The value of \bar{P} is 0.26, much higher than that for the previous case, and a substantial fraction of the Landau-Zener maximum.

$Ne^{5+} + He$ (Fig. 4). The favored Q value now falls in the midst of a large number of unresolved states built by the addition of an $n=3$ electron to the projectile core. The experimental peak is substantially broader than the resolution function, showing that the capture strength is shared among $3d$ and $3p$ states; little evidence for $3s$ population is seen. There appears to be some shift of the centroid toward population of the more weakly bound $3d$ states as the projectile energy is decreased, as would be expected from the diabaticity arguments given above. Unfortunately, the angular cutoff acts in the same direction, and thus unambiguous interpretation of this effect is not possible. The value of \bar{P} obtained for an average crossing radius at 3.2 Å is 0.52, slightly larger than the maximum Landau-Zener value.

$Ne^{6+} + He$ (Fig. 5). This is a particularly interesting transition case. The population of even the $3d$ state has now become so exoergic that the corresponding crossing radius is far inside R_f . The $n=4$ states, on the other hand, involve quite distant crossings substantially outside R_f . There are many states near the favored Q , but these are all based on a $2s2p$ excited core, and thus are only weakly coupled to the incident channel involving a $(2s^2)^1S$ projectile. The result, as seen in Fig. 5(a), is that no clear-cut favorite emerges. Substantial $3d$ population is still present, with a \bar{P} of 0.44, but the total cross section still is smaller than that for either $+5$ or $+7$ projectiles due to the small crossing radius for this channel. This result is in agreement with that of Gordeev *et al.*²⁹ who find strong emission from $3d$ levels in this reaction at higher projectile velocities.

As the acceleration voltage is lowered to 222.7 eV [Fig. 5(b)], apparent population of the core excited states increases at the expense of the $3d$ population, as would be expected from the v dependence of R_f in the model discussed above. This effect becomes even more marked at $V_{acc}=124.2$ and 72.4 eV [Figs. 5(c) and 5(d)], but is at least partially due to loss of $3d$ events because of the angular cutoff.

$Ne^{7+} + He$ (Fig. 6). The population of $n=4$ is favored and observed to dominate the spectra. The value of \bar{P} for this population is 0.21. An additional group appears with a Q value near 35 eV and an intensity of approximately 15% of the $n=4$ single-capture intensity [Figs. 6(a)–6(c)]. We interpret this group as due to the population by double capture of a group of doubly excited states with $(n,n')=(3,4)$. Evidence for this process has been previously seen for C^{7+} and N^{7+} on He by Tsurubuchi *et al.*¹³ and Tawara *et al.*¹⁴ In the present case, no theoretical calculations of the energies of the doubly excited states are available. We have estimated the centroids of expected groups from the known experimental binding energies of $n=3$ and $n=4$ electrons in singly excited states based on a Ne^{7+} ground-state core.²⁶ There is extensive multiplet splitting to be expected about this centroid, however, and identification of individual states is

not possible. The previous work of Justiniano *et al.*²⁴ showed a transfer ionization cross section for Ne^{7+} on He at $V_{acc}=500$ V which was approximately 13% of the single-capture cross section, consistent with the present interpretation.

Energy-gain spectra at $V_{acc}=1$ kV have been reported for this system by Tawara *et al.*,¹⁴ who found population of groups with Q values of 20, 38, and 68 eV in agreement with the present results. They interpret the group at 38 eV as due to population of $(2p3l)$ core excited states in single capture; this interpretation cannot be excluded. We prefer the transfer ionization interpretation, however, in view of the results of Justiniano *et al.*²⁴ and the fact that our systematics seem to show that the population of core-excited states away from the favored Q region is improbable. The group at 68 eV, which appears clearly only in Fig. 6(b), is attributed to transfer ionization to $(n,n')=(3l,nl')$. Evidence for population of this channel also appears in their spectrum for F^{7+} on He. Double capture to final Ne^{5+} states are outside the voltage ranges scanned for the figures displayed.

$Ne^{8+} + He$ (Fig. 7). Capture to $n=4$ continues to dominate for this case with $\bar{P}=0.55$. A group with Q near 48 eV is also populated, and probably due to double capture to $(n,n')=(3,4)$ again, although the kinematic shift is large and renders unique identification of this group difficult. In addition, it is not clear whether the electron emission occurs during the capture process or afterwards from decaying doubly excited states, which also effects the position and width of those peaks. This identification is consistent with the results of Justiniano *et al.*,²⁴ who found population of a transfer ionization channel with an intensity of 20% of the single capture. This group is not resolved in the spectra of Tawara *et al.*¹⁴

Ne^{9+} and $Ne^{10+} + He$. These systems have been studied previously by Mann *et al.*¹⁶ and by Tawara *et al.*;¹⁴ their properties are summarized here for completeness. For Ne^{9+} on He, the population shifts to $n=5$, but the favored crossing radius is inside the actual crossing with $n=5$, with the result that a rather low value of $\bar{P}=0.15$ is obtained. Their cross section for this case is less than that for either Ne^{8+} or Ne^{10+} projectiles. For Ne^{10+} on He, the cross section rises, as the $n=5$ crossing radius is now quite close to R_f , and \bar{P} rises to 0.27.

IV. CONCLUSIONS

The present results indicate that the energy balance of the capture reaction is the most important parameter in determining which levels are most strongly populated in the process. If curve crossings occur for which the strength of the potential coupling between incident and final channels is optimized, those states will be selectively populated. A simple prescription for calculating the favored internuclear radius, or the corresponding favored Q value, does remarkably well at predicting which states will be selected. Although the prescription given by Eqs. (1) and (2) is based on a very simplified two-level Landau-Zener analysis, nearly the same results for the favored radii can be obtained by taking the absorption radius described for the many-crossing case by Olson and

Salop. This result occurs because H_{12} is so steeply R dependent. The favored radius idea is very similar to that of a "reaction window" discussed by several authors^{14,30-34} which favors crossings occurring between about 2.5 and 5 Å. In the present prescription, the favored radius is system dependent.

For cases where configurations based on the projectile ground-state core have crossings near the favored radius ($\text{Ne}^{4+,5+,7+,8+,10+}$), population of those configurations is selected. For cases where crossings with favored configurations lie sufficiently far from the favored radius ($\text{Ne}^{3+,6+}$), population of core excited configurations becomes competitive. It appears that the steep dependence of the coupling matrix element on R has the result that having a crossing at the favored R can be more crucial than having the right configuration. In particular, no favoring of any l , within a given n manifold, is found except as dictated by the energetics. For example, for Ne^{4+} , $3s$ states are selected, while for Ne^{5+} $3p$ and $3d$ states are preferred. This difference is directly attributable to the proximity of the populated levels to the favored Q value.

It is possible that our beams have, in some cases, metastable components which can lead to the population of systems which have not been considered in the discussion. However, the binding energy of a single $n=3$ (or higher) electron to a metastable core will differ little in most cases from that to the ground state. Thus the energy balance for capturing into a particular n will be nearly independent of the excitation level of the core, if the core does not change its electronic energy in the collision, and the discussion based on the assumption of a ground-state projectile core remains approximately valid.

Except for the transition cases of Ne^{3+} and Ne^{6+} , tran-

sitions to a single group of levels dominates the transfer, and a semiquantitative interpretation of the average transition probability \bar{P} is possible. Since in every case several channels are being fed, one might expect the absorption value of $\bar{P} \approx 1.0$ to be obtained. This does not occur, as our experimental \bar{P} never exceeds 0.55 for the most favored case (Ne^{8+}). In a simplified model in which both projectile and target are taken to be point charges, the latter clothed by a single electron, only a single level out of a given n manifold couples to the incident channel, and this apparent multicrossing case is really only a two-level case. It is not clear to what extent such a model approximates reality for a case where the subshell degeneracy is lifted. If one views the coupling of many levels with $n=3$ as really only a single coupling to that linear combination of states with different l which couples to the incident channel, the Landau-Zener result that \bar{P} maximizes at 0.52 is quite consistent with the present results. We note that other authors have reported cross sections up to nearly 100% of πR_c^2 , corresponding to \bar{P} of unity, for similar systems.^{12,14} We do not find this. It is perhaps the case that in order to really satisfy the multilevel approximation, the density of states with different n near the favored radius must be high. Such is the case for, for example, a Li target, for which the absorbing sphere model was found to work well.²⁵

ACKNOWLEDGMENTS

This work was supported by the Division of Chemical Sciences of the U.S. Department of Energy. One of us (W.E.M.) is supported by the National Science Foundation under Grant No. PHY-83-13676.

*Permanent Address: Gesellschaft für Schwerionenforschung, D-6100 Darmstadt 11, West Germany.

¹D. H. Crandall, R. E. Olson, E. Salzborn, A. Müller, F. J. deHeer, M. Panpov, H. Ryufuku, and T. Watanabe, in *Proceedings of the Eleventh International Conference on the Physics of Electronic and Atomic Collisions, Kyoto, 1979*, edited by N. Oda and K. Takayanagi (North-Holland, Amsterdam, 1980), p. 398.

²P. Hvelplund, H. Knudsen, C. L. Cocke, R. Mann, Y. Kaneko, and M. Gargaud, in *Proceedings of the Twelfth International Conference on the Physics of Electronic and Atomic Collisions, Gatlinburg, Tennessee, 1981*, edited by S. Datz (North-Holland, Amsterdam, 1982), p. 655.

³R. K. Janev, *Comments At. Mol. Phys.* **12**, 277 (1983).

⁴*Proceedings of the International Conference on the Production and Physics of Highly Charged Ions*, edited by L. Lilejby [Phys. Scr. **T3**, (1983)].

⁵*Atomic and Molecular Processes in Thermonuclear Fusion*, Vol. 53 of *NATO Advanced Study Institute Series B*, edited by M. K. C. McDowell and A. M. Ferendici (Plenum, New York, 1980).

⁶*Atomic and Molecular Data for Fusion*, edited by H. W. Drawin and K. Katsonis [Phys. Scr. **23**, (1981)].

⁷R. Mann, F. Folkmann, and H. F. Beyer, *J. Phys. B* **14**, 1161 (1981).

⁸H. F. Beyer, K. H. Schartner, and F. Folkmann, *J. Phys. B* **13**, 2459 (1980).

⁹S. Bliman, M. Bonnefoy, J. J. Bonnet, S. Dousson, A. Fleury, D. Hitz, and B. Jacquot, *Phys. Scr.* **T3**, 63 (1983).

¹⁰D. Dijkkamp, R. L. Vander Woude, F. J. deHeer, A. G. Drentje, A. Barazuk, and H. Winter, *Phys. Scr.* **T3**, 551 (1983).

¹¹Yu. S. Gordeev, D. Dijkkamp, A. G. Drentje, and F. J. deHeer, *Phys. Rev. Lett.* **50**, 1842 (1983).

¹²S. Ohtani, Y. Kaneko, M. Kimura, M. Kobayashi, T. Iwai, A. Matsumoto, K. Okuno, S. Takagi, H. Tawara, and S. Tsurubuchi, *J. Phys. B* **15**, L533 (1982).

¹³S. Tsurubuchi, T. Iwai, Y. Kaneko, M. Kimura, N. Kobayashi, A. Matsumoto, S. Ohtani, K. Okuno, S. Takagi, and H. Tawara, *J. Phys. B* **15**, L733 (1982).

¹⁴H. Tawara, T. Iwai, Y. Kaneko, M. Kimura, N. Kobayashi, A. Matsumoto, S. Ohtani, K. Okuno, S. Takagi, and S. Tsurubuchi, *Phys. Rev. A* **29**, 1529 (1984).

¹⁵K. Okuno, H. Tawara, T. Iwai, Y. Kaneko, M. Kimura, N. Kobayashi, A. Matsumoto, S. Ohtani, S. Takagi, and S. Tsurubuchi, *Phys. Rev. A* **28**, 127 (1983).

- ¹⁶R. Mann, C. L. Cocke, A. S. Schlachter, M. Prior, and R. Marrus, *Phys. Rev. Lett.* **49**, 1324 (1982).
- ¹⁷B. A. Huber, *Phys. Scr.* **T3**, 96 (1983).
- ¹⁸H. J. Kahlert, B. A. Huber, and K. Wiesmann, *J. Phys. B* **16**, 4491 (1983).
- ¹⁹B. A. Huber and H. J. Kahlert, *J. Phys. B* **16**, 4655 (1983).
- ²⁰E. Y. Kamber and J. B. Hasted, *J. Phys. B* **16**, 3025 (1983).
- ²¹E. H. Nielsen, L. H. Andersen, A. Barany, H. Cederquist, P. Hvelplund, H. Knudsen, K. B. MacAdam, and J. Sorensen, *J. Phys. B* (to be published).
- ²²H. Ryufuku, K. Sasaki, and T. Watanabe, *Phys. Rev. A* **21**, 745 (1980).
- ²³E. Justiniano, C. L. Cocke, T. J. Gray, R. D. Dubois, and C. Can, *Phys. Rev. A* **24**, 2953 (1981).
- ²⁴E. Justiniano, C. L. Cocke, T. J. Cray, R. Dubois, C. Can, W. Waggoner, R. Schush, H. Schmidt-Böcking, and H. Ingwersen, *Phys. Rev. A* **29**, 1088 (1984).
- ²⁵S. Bashkin and J. O. Stoner, Jr., *Atomic Energy Levels and Grotrian Diagrams* (North-Holland, Amsterdam, 1975).
- ²⁶C. E. Moore, *Atomic Energy Levels*, Natl. Bur. Stand. (U.S.) No. 467 (U.S. GPO, Washington, D.C., 1952).
- ²⁷C. Zener, *Proc. R. Soc. London, Ser. A* **137**, 696 (1932).
- ²⁸R. Olson and A. Salop, *Phys. Rev. A* **14**, 579 (1976).
- ²⁹Yu. S. Gordeev, D. Dijkkamp, A. G. Drentje, and F. J. deHeer, *Phys. Rev. Lett.* **50**, 1842 (1983).
- ³⁰H. Winter, E. Bloemen, and F. J. deHeer, *J. Phys. B* **10**, L599 (1977).
- ³¹B. A. Huber, *Phys. Scr.* **T3**, 96 (1983).
- ³²W. Lindinger, *Phys. Scr.* **T3**, 115 (1983).
- ³³S. Ohtani, *Phys. Scr.* **T3**, 110 (1983).
- ³⁴D. Smith, N. G. Adams, E. Alge, H. Villinger, and W. Lindinger, *J. Phys. B* **13**, 2787 (1980).
- ³⁵W. Waggoner, C. L. Cocke, S. L. Varghese, and M. Stockli, *Phys. Rev. A* **29**, 2457 (1984).
- ³⁶E. Justiniano, Ph.D. thesis, Kansas State University, 1982.